Diagnostic ability of Humphrey perimetry, Octopus perimetry, and optical coherence tomography for glaucomatous optic neuropathy

B Monsalve[1,2], A Ferreras[3,4], P Calvo[3,4], JA Urcola[5], M Figus[6], J Monsalve[2] and P Frezzotti[7]

CLINICAL STUDY

Abstract

Purpose To evaluate and compare the diagnostic accuracy of the Humphrey Field Analyzer (HFA), Octopus perimetry, and Cirrus OCT for glaucomatous optic neuropathy.
Methods Eighty-eight healthy individuals and 150 open-angle glaucoma patients were consecutive and prospectively selected. Eligibility criteria for the glaucoma group were intraocular pressure ≥ 21 mm Hg and glaucomatous optic nerve head morphology. All subjects underwent a reliable standard automated perimetry with the HFA and Octopus perimeter, and were imaged with the Cirrus OCT. Receiver-operating characteristic (ROC) curves were plotted for the threshold values and main indices of the HFA and Octopus, the peripapillary retinal nerve fiber layer thicknesses, and the optic nerve head parameters. Sensitivities at 85 and 95% fixed-specificities were also calculated. The best areas under the ROC curves (AUCs) were compared using the DeLong method.
Results In the glaucoma group, mean deviation (MD) was -5.42 ± 4.6 dB for HFA and 3.90 ± 3.6 dB for Octopus. The MD of the HFA (0.966; $P < 0.001$), mean sensitivity of the Octopus (0.941; $P < 0.001$), and average cup-to-disc (C/D) ratio measured by the Cirrus OCT (0.958; $P < 0.001$) had the largest AUCs for each test studied. There were no significant differences among them. Sensitivities at 95% fixed-specificity were 82% for pattern standard deviation of the HFA, 81.3% for average C/D ratio of OCT, and 80% for the MD of the Octopus.
Conclusions HFA, Octopus, and Cirrus OCT demonstrated similar diagnostic accuracies for glaucomatous optic neuropathy. Visual field and OCT provide supplementary information and thus these tests are not interchangeable.

Introduction

Primary open-angle glaucoma is generally considered a progressive optic neuropathy, including damage at the optic nerve head (ONH) and/or retinal nerve fiber layer (RNFL), and reduced visual function.[1] Randomized clinical trials indicate that the first detectable glaucomatous change at early stages of the disease can be either functional or structural.[2,3] The agreement among RNFL, neuroretinal rim, and visual field (VF) measurements for detecting progression, however, is poor,[4–6] and a combination of structural and functional tests is therefore used to increase the diagnostic sensitivity and detection of progression.[7,8]

Standard automated perimetry (SAP) has become the functional clinical standard for diagnosing and monitoring patients with glaucoma. Particularly, the 24-2 Swedish Interactive Threshold Algorithm (SITA) of the Humphrey Field Analyzer (HFA)[9] and the G1 Tendency-Oriented Perimetry strategy (TOP) of the Octopus[10] are among the most commonly used VF algorithms worldwide. Objective structural imaging instruments have also been standardized for the diagnosis and follow-up of patients with, or at risk for, glaucoma. One of these tools is optical coherence tomography (OCT), which provides quantitative and reproducible measurements of the ONH parameters and peripapillary RNFL

[1]Department of Ophthalmology, Hospital General Universitario Gregorio Marañón, Instituto Oftálmico de Madrid, Madrid, Spain

[2]Department of Ophthalmology, Hospital Moncloa, Oftalvist, Madrid, Spain

[3]Department of Ophthalmology, Miguel Servet University Hospital, IIS Aragon, Zaragoza, Spain

[4]Department of Surgery, Gynecology and Obstetrics, University of Zaragoza, Zaragoza, Spain

[5]Department of Ophthalmology, Hospital Universitario Araba, Vitoria, Spain

[6]Department of Neurosciences, University of Pisa, Pisa, Italy

[7]Department of Ophthalmology, University of Siena, Siena, Italy

Correspondence:
A Ferreras, Department of Ophthalmology, Miguel Servet University Hospital, Isabel la Catolica 1-3, Zaragoza 50009, Spain
Tel: +34 976765558;
Fax: +34 976566234.
E mail: aferreras@msn.com

thickness.[11–15] Understanding their comparative roles and performance in clinical practice is key to the management of glaucoma.

Current knowledge of the relative diagnostic performance of both SAPs (HFA and Octopus) and OCT comes from studies in which the data were analyzed independently for each test or where only one kind of SAP was compared with a structural test.[11–20] Some studies compared tests for evaluating the VF based on other stimuli than white-on-white perimetry,[21–27] or evaluated the structure–function relationship.[28–33] The objective of the present study was to evaluate and compare the glaucoma diagnostic accuracy of the most widely used VF testing algorithms in clinical practice (24-2 SITA Standard strategy of HFA and G1 TOP strategy of Octopus) with one of the most advanced structural imagining tests (OCT). To the best of our knowledge, this is the first study aimed at comparing the diagnostic accuracy of these tests.

Materials and methods

Participants

The Institutional Review Board approved the prospective study protocol. All participants provided informed consent prior to enrollment and the study methodology adhered to the tenets of the Helsinki Declaration for biomedical research.

A sample of 249 consecutive subjects was prospectively preselected. Glaucoma patients were recruited from the Department of Ophthalmology of the Gregorio Maranon University Hospital and the Glaucoma Clinic of the Moncloa Hospital (Madrid, Spain). Controls were enrolled from patients referred for refraction without abnormal ocular findings, relatives of patients, and friends and family of the hospital staff.

Inclusion criteria for the glaucoma group were a glaucomatous optic disc morphology and intraocular pressure (IOP) ≥ 21 mm Hg, regardless of the SAP or OCT outcomes. The control group had normal optic disc morphology and IOP < 21 mm Hg.

The morphology of the ONH was evaluated by slit-lamp indirect ophthalmoscopy with a 90-diopter lens. The optic discs were evaluated by two glaucoma specialists masked to patient identity and clinical history, and any disagreement was resolved by consensus. Glaucomatous optic disc appearance was defined as focal (localized notching) or diffuse neuroretinal rim narrowing with concentric enlargement of the optic cup or both.

All participants met the following inclusion criteria: best-corrected visual acuity $> 20/40$, refractive error < 5 D sphere and 2 cylinder, transparent ocular media (nuclear color/opalescence, cortical or posterior

subcapsular lens opacity < 1) according to the Lens Opacities Classification System III system,[34] and open anterior chamber angle. Subjects with previous intraocular surgery, diabetes or other systemic diseases, history of ocular or neurologic disease, or current use of a medication that could affect VF sensitivity were excluded.

Participants underwent full ophthalmologic examination: clinical history, visual acuity, biomicroscopy of the anterior segment using a slit lamp, gonioscopy, Goldmann applanation tonometry, central corneal ultrasonic pachymetry, and ophthalmoscopy of the posterior segment.

Visual field measurements

All participants underwent at least two white-on-white SAPs with the HFA (Humphrey Zeiss Systems, Dublin, CA, USA; 24-2 SITA Standard strategy) and at least two SAPs with the Octopus (Haag-Streit International, Koeniz, Switzerland; G1 TOP test strategy) to minimize the learning effect. If the perimetry was not reliable (fixation losses $< 20\%$ and false positive and negative rates $< 15\%$), the test was repeated. The last reliable perimetry was included in the statistical analysis. The subjects completed the perimetry tests before undergoing clinical examination or structural testing. Each perimetry examination was performed on different days to avoid a fatigue effect.

HFA and Octopus perimeters use the same background lighting of 31.5 apostilbs (asb). Retinal sensitivity measured by both perimetry types is indicated in decibels (dB), which are tenths of a log unit. Nonetheless, the maximal luminance varied between the instruments. A 0 dB value was the maximum brightness, which corresponds to a 10 000 asb stimulus intensity for HFA, and 4000 asb for Octopus perimetry.

OCT measurements

Peripapillary RNFL thickness and optic disc morphometric parameters were measured using the Optic Disc Cube 200×200 scanning protocol of the Cirrus OCT (Carl Zeiss Meditec). For image acquisition, scanning laser images were focused after subjects were seated and properly positioned. The left eye data were converted to a right eye format (Figure 1). All images were artifact-free and acquired with a quality greater than $> 6/10$. The same trained operator performed all scans.

Statistical analyses

All statistical analyses were calculated using SPSS for Mac (version 22.0, IBM corporation, Somers, NY, USA) and Windows MedCal statistical software (version 15; Mariakerke, Belgium). Minimum sample size should be
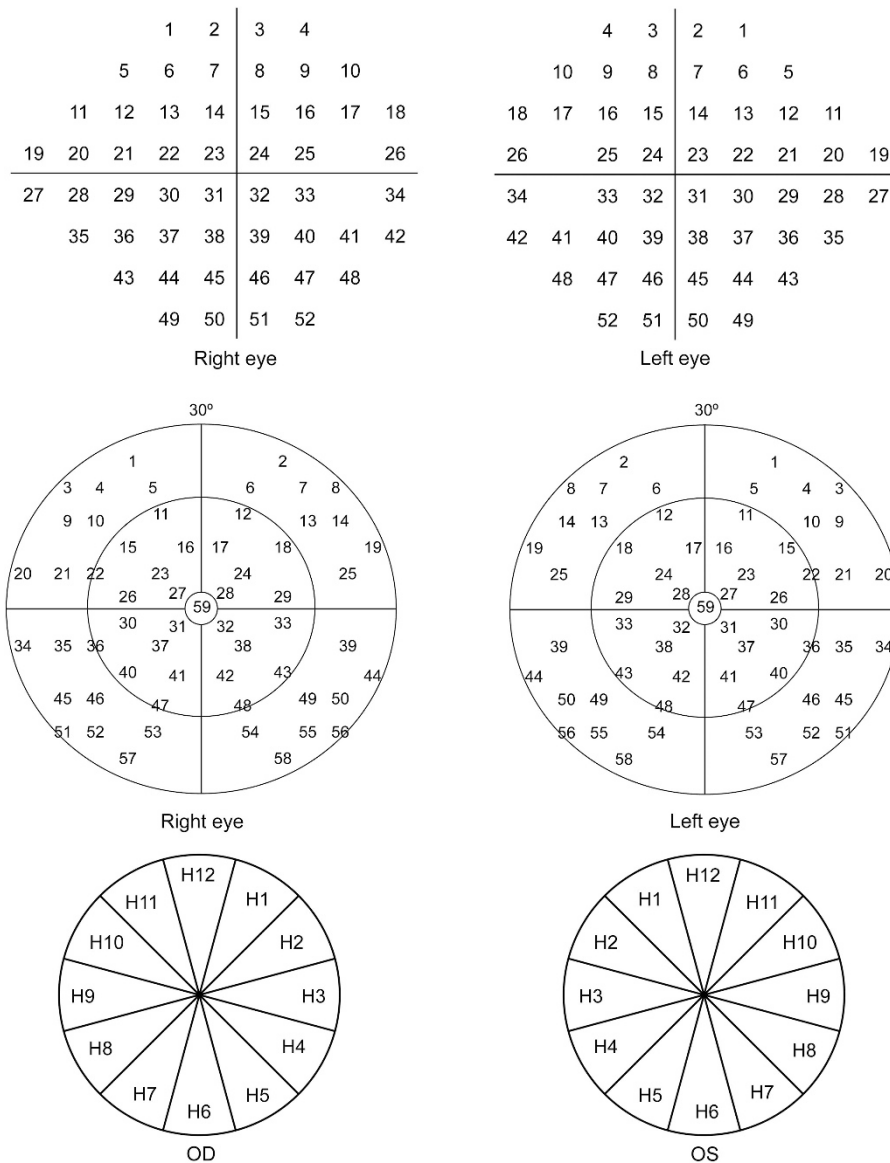
Figure 1 The grid of HFA was numbered as shown at the top, while each of the test points of the Octopus was numbered as shown in the middle. Bottom: The 12 OCT sectors were numbered according to the 12 clock-hour positions.

eight individuals per group considering a difference of 25.1 μm for the average thickness as significant,[14] with a type 1 error rate of 0.01, and a power of 90%. All variables studied were normally distributed, as verified by the Kolmogorov–Smirnov test. Demographics, HFA, Octopus, and OCT parameters were compared between groups with independent *t*-tests.

Each of the mean threshold values at each point of the VF was numbered (Figure 1). To evaluate the diagnostic ability for glaucoma, the receiver-operating characteristic (ROC) curves were plotted for the RNFL and ONH parameters acquired with OCT, and for all the HFA and Octopus study points and main parameters. Sensitivities at 85 and 95% fixed-specificities were also calculated. The best areas under the ROC curves (AUCs) were compared using the DeLong method, which is an algorithm for the calculation of the standard error of the AUC and of the difference between two AUCs.[35] Using Bonferroni's correction for multiple comparisons, a *P*-value ≤ 0.001 was considered significant.

Data availability

The data that support the findings of this study are available from the corresponding author upon reasonable request.

Results

Of the 249 enrolled participants, 11 did not complete all required tests and were excluded from further analysis. In total, 150 eyes of 150 glaucoma patients and 88 eyes of 88 healthy subjects were enrolled. Their clinical characteristics are summarized in Table 1. Comparison of the clinical characteristics revealed significant differences ($P < 0.001$) in all the parameters except age, sex, and laterality of eye included.

Among the 150 glaucoma participants, 24 had normal HFA results according to pattern standard deviation (PSD) or the glaucoma hemifield test. Three participants of the control group presented with PSD beyond 5% probability level. This finding can be explained as part of the VF learning process. Among the 150 glaucoma participants, 32 had normal Octopus results based on mean deviation (MD < 2 dB). All the controls had normal Octopus results.

Figure 2 represents the mean sensitivity (MS) at each study point of the VF evaluated with the HFA and Octopus in the two study groups. There was a clear depression of the sensitivity at all points of the VF in the glaucoma group, which was especially significant in the area corresponding to the upper arcuate defects and nasal step (orange-red color in HFA and yellow-orange in Octopus). All threshold values of both the HFA and Octopus were significantly different ($P < 0.001$) between normal subjects and the glaucoma group (Student's *t*-test).

All peripapillary RNFL thickness and ONH parameters measured with OCT were significantly different between healthy and glaucoma patients, except for at the 3 (nasal sector; $P = 0.306$) and 9 clock-hour positions (temporal sector; $P = 0.035$), and the disc area ($P = 0.536$).

Diagnostic ability of the RNFL thickness and ONH parameters measured by OCT

To evaluate the diagnostic ability for glaucoma of the three studied tests, the AUCs were calculated with their 95% confidence intervals. AUCs of the RNFL thickness measurements and ONH parameters measured by OCT are presented in Figure 3 (bottom). Among these parameters, Mean cup-to-disc (C/D) ratio had the largest AUC (0.958; 95% CI: 0.937–0.980; $P < 0.001$), followed by the Vertical C/D ratio (0.957; 95% CI: 0.935–0.978; $P < 0.001$), and Rim area (0.952; 95% CI: 0.927–0.977; $P < 0.001$). Except for the Disc area (0.513; 95% CI: 0.437–0.587; $P = 0.74$), all parameters had AUCs > 0.90 ($P < 0.001$).

The RNFL thicknesses showed good diagnostic ability in the superior and inferior quadrants and 5–7 and 11–2 clock-hour positions (AUCs > 0.774; $P < 0.001$). The AUCs of the RNFL thickness in the nasal and temporal quadrants, and at the 3, 4, and 8 to 10 clock-hour positions, however, ranged from 0.599 to 0.710 (Figure 3). The inferior quadrant thickness (0.926; 95% CI: 0.894–0.958; $P < 0.001$), Mean thickness (0.918; 95% CI: 0.885–0.952; $P < 0.001$), and RNFL thickness at the 7 clock-hour position (0.905; 95% CI: 0.869–0.940; $P < 0,001$) had the largest AUCs.
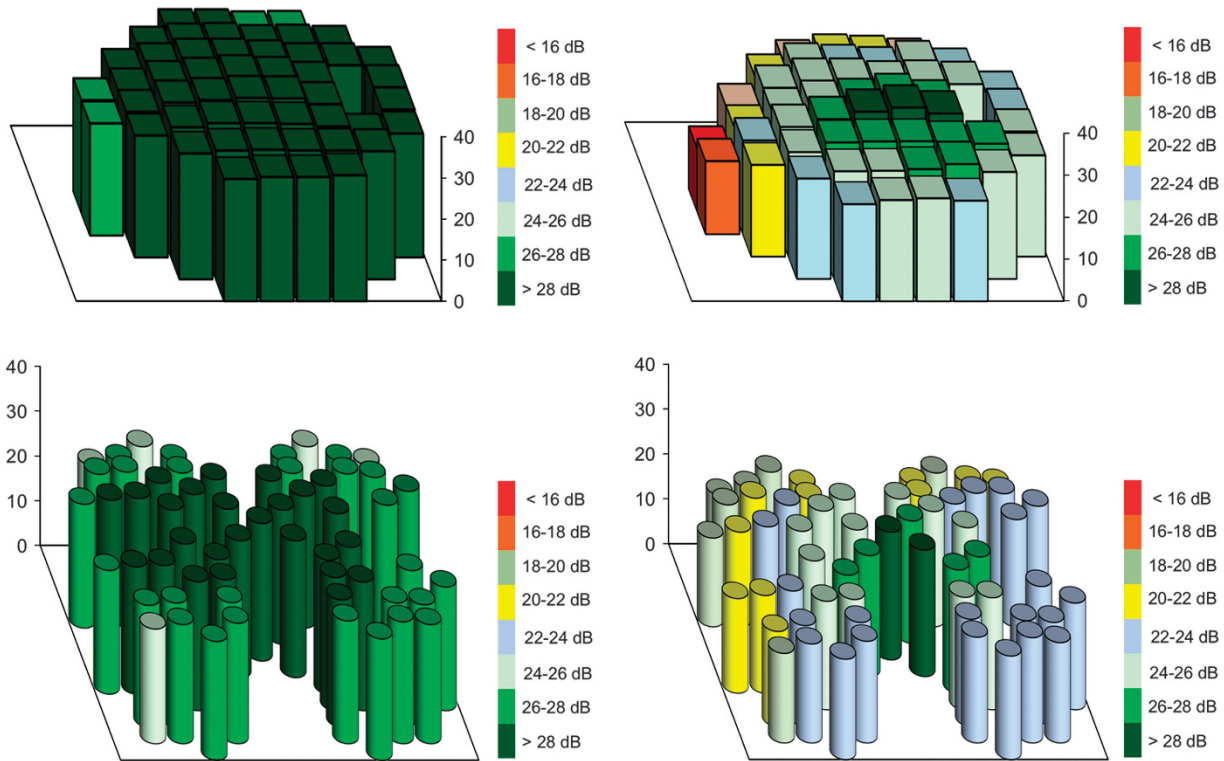
Diagnostic ability of HFA

Figure 3 (top and right) represents the AUCs of the main HFA indices. The largest AUCs were observed for the MD (0.966; 95% CI: 0.945–0.987; $P < 0.001$) and VF index (VFI) (0.961; 95% CI: 0.934–0.987; $P < 0.001$). The largest AUCs were found for the threshold values at point 7 (0.901; 95%

Table 1 Demographic characteristics of the study population.

	Healthy group				Glaucoma group				P-value
	Minimum	Maximum	Mean	SD	Minimum	Maximum	Mean	SD	
Age (years)	39	79	57.58	8.69	27	80	59.46	9.81	0.125
BCVA (Snellen)	0.6	1	0.95	0.10	0.5	1	0.88	0.16	**<0.001**
Baseline IOP (mm Hg)	9	21	15.77	2.92	22	46	25.38	4.84	**<0.001**
CCT (μm)	453	629	551.02	35.43	445	638	535.82	39.42	0.001
C/D	0.1	0.5	0.44	0.17	0.4	0.9	0.73	0.12	**<0.001**
MD HFA (dB)	-1.65	2.57	0.60	1.01	-22.11	1	-5.42	4.62	**<0.001**
PSD HFA	0.88	4.17	1.51	0.44	1.19	14.2	5.89	3.64	**<0.001**
VFI HFA	96	100	99.53	0.80	28	100	87.92	12.21	**<0.001**
MS Octopus (dB)	25.1	29.8	27.89	1.06	11	28.5	23.07	3.66	**<0.001**
MD Octopus (dB)	-2.6	2.4	-0.61	0.96	-1.6	15.5	3.90	3.55	**<0.001**
sLV Octopus (dB)	0.3	9.7	2.55	1.60	1.18	10.88	4.03	2.12	**<0.001**
n	88				150				

Abbreviations: BCVA, best-corrected visual acuity; CCT, central corneal thickness; C/D, vertical cup-to-disc ratio; HFA, Humphrey field analyzer; IOP, intraocular pressure; MD, mean deviation; MS, Mean sensitivity; n, number of cases; PSD, pattern standard deviation; sLV, square root of loss variance; VFI, visual field index.
Statistically significant differences are highlighted in bold ($P < 0.001$).

Figure 2 Mean threshold values at each study point of the HFA and Octopus perimetries. Top: HFA perimetry; Bottom: Octopus perimetry. The control and glaucoma groups are represented on the left and right sides, respectively.

CI: 0.857–0.944; $P < 0.001$), point 19 (0.911; 95% CI: 0.867–0.954; $P < 0.001$), point 20 (0.923; 95% CI: 0.886–00.961; $P < 0.001$), and point 21 (0.914; 95% CI: 0.875–0.954; $P < 0.001$).

Diagnostic ability of Octopus Perimetry

Figure 3 (top and left) represents the AUCs of the main Octopus indices. The largest AUCs were observed for MS (0.941; 95% CI: 0.913–0.969; $P < 0.001$). The largest AUCs were observed for the threshold values at point 3 (0.907; 95% CI: 0.870–0.944; $P < 0.001$), point 5 (0.900; 95% CI: 0.861–0.940; $P < 0.001$) and point 21 (0.911; 95% CI: 0.877–0.946; $P < 0.001$).

### Comparison of the diagnostic ability between the HFA, Octopus, and OCT

Overall, the best sensitivity/specificity balance was observed for the VFI of HFA (91.3–89.8%; cutoff point ≤98) and the PSD of HFA (87.3–93.2%; cutoff point >1.88). The Octopus parameter with the best sensitivity-specificity balance was MD (84.6–94.3%; cutoff point >0.75). Table 2 represents sensitivities at 85 and 95% fixed-specificities. At 85% fixed-specificity, the best

parameter for discriminating between control and glaucoma patients was the VFI of HFA (93.3%), and at 95% fixed-specificity the best parameter to discriminate between control and glaucoma eyes was the PSD of HFA (82.0%).

The comparison of the best AUCs (DeLong method) of the three-study test did not show significant differences between them. No differences were detected (significant differences were considered when $P \le 0.001$) between the MD of the HFA and the MS of the Octopus ($P = 0.042$), or between the MD of the HFA and RNFL thickness at the inferior quadrant ($P = 0.027$).

Discussion

Our study was designed to assess and compare the diagnostic accuracy of the 24-2 SITA-Standard algorithm of HFA, the G1 TOP strategy of the Octopus, and OCT to discriminate between normal and glaucoma patients. The best parameter to discriminate between healthy and glaucoma eyes at 95% fixed specificity was the PSD of the HFA (sensitivity 82.0%). Additionally, HFA parameters presented better numerical AUCs than the Octopus and OCT parameters, but comparison of the ROC curves
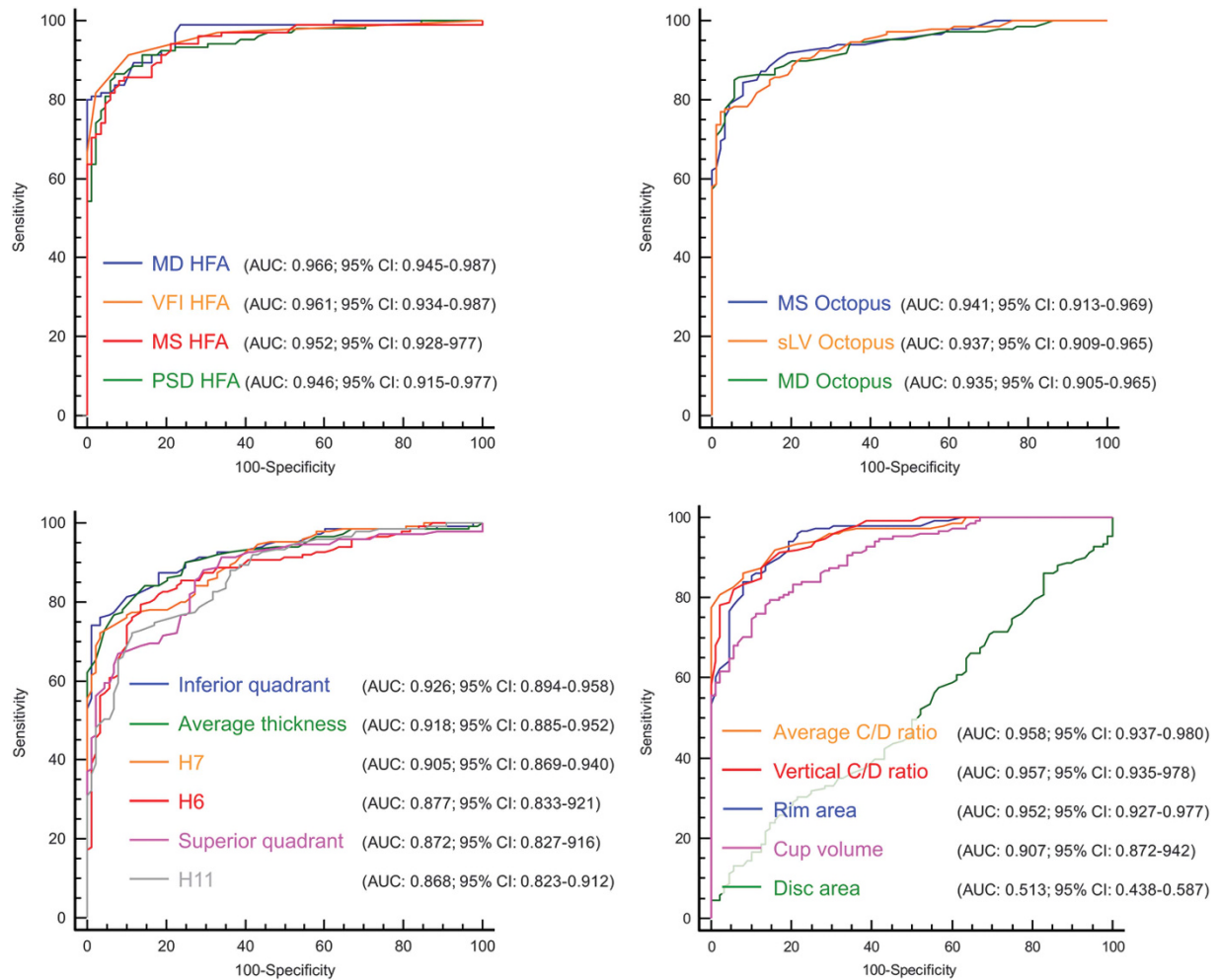
Figure 3 Top: area under the ROC curves of the main HFA (left) and Octopus (right) parameters. Bottom: area under the ROC curves of the best RNFL parameters (left) and of the optic disc morphometric parameters (right) measured by Cirrus OCT. H = RNFL thickness at clock hour position for a right eye.

revealed no significant differences in the diagnostic ability of the three tests. Nevertheless, the $P < 0.001$ condition for statistical significance was set high due to multiple comparisons, and this fact is actually limiting the ability to compare the tests. Although the DeLong method did not show significant differences, we should take into account that the low P-values are suggestive of a difference, even if they do not reach the fixed level to be considered as significant in this study.

The main parameters of the HFA and Octopus (Figure 3, top) had good accuracy for discriminating between normal and glaucoma eyes (all AUCs > 0.929; $P < 0.001$). The VF parameters with the best AUCs were MD of the HFA (0.966; 95% CI: 0.945–0.987; $P < 0.001$) and MS of the Octopus (0.941; 95% CI: 0.913–0.969; $P < 0.001$). Our inclusion criteria were very strict and only included

participants with transparent ocular media. This fact may have led to these results, where the MD of the HFA and the MS of the Octopus had larger AUCs than PSD of the HFA and square root of loss of variance (sLV) of the Octopus, which are usually more sensitive for detecting focal losses instead of diffuse vision loss. The study population was selected to avoid any other ocular pathologies than glaucoma in the glaucoma group. Participants presented with very good visual acuities, no cataracts, and no previous intraocular surgeries.

We found similar sensitivities at fixed specificities for the main indices of the Octopus. In a study published in 2006 by De la Rosa *et al*[18] analyzing the diagnostic accuracy and reproducibility of TOP in glaucoma, the Octopus MD and Octopus LV had similar diagnostic precision for moderate and advanced

Table 2 Sensitivities at 85 and 95% fixed-specificities.

	Specificity 85%	Specificity 95%
Cirrus H7	78.0%	75.3%
RNFL average thickness	85.3%	75.3%
Inferior quadrant	83.3%	76.0%
Average C/D	91.3%	81.3%
MD HFA	91.3%	81.3%
PSD HFA	90.0%	**82.0%**
VFI HFA	**93.3%**	80.0%
MS HFA	85.3%	80.0%
HFA 7	78.7%	62.7%
HFA 19	85.3%	68.7%
HFA 20	84.0%	72.0%
HFA 21	81.3%	66.7%
MS Octopus	89.3%	78.7%
MD Octopus	86.0%	80.0%
sLV Octopus	85.3%	78.0%
Octopus 3	83.3%	70.7%
Octopus 21	83.3%	80.0%

Abbreviations: C/D, cup-to-disc-ratio; H, clock-hour position; HFA, Humphrey Field Analyzer; MD, mean deviation; MS, mean sensitivity; PSD, pattern standard deviation; RNFL, retinal nerve fiber layer; sLV, square root of loss variance; VFI, visual field index.
The best sensitivities are highlighted in bold.

glaucoma, but the LV was the best diagnostic index when the MD was <6 dB.

The largest AUCs were for the MD of the HFA (0.966; 95% CI: 0.945–0.987; $P < 0,001$) and the VFI of the HFA (0.961; 95% CI: 0.934–0.987; $P < 0.001$). Although the VFI presented the best sensitivity/specificity balance and the best sensitivity (93%) at 85% fixed specificity, clinicians should take into account the ceiling effect that occurs in VFI with MDs better than − 5 dB.[36]

Study points with the largest AUCs were located in the superior hemifield: points 7, 19, 20, and 21 of the HFA, and points 3 and 21 of the Octopus. These study points represent a superior arcuate defect and a nasal step, locations of very typical glaucomatous VF defects.[37–39] Paracentral points (19 and 10) have also been documented as very typical of glaucoma, especially when regionally enhanced spatial resolution is used,[40] but points close to the fovea did not present with good AUCs in our sample (mild glaucoma). We used non-equivalent strategies from both perimetry types, SITA Standard and TOP, because they are the default strategies used in clinical practice. Our objective was to analyze the strategies that are normally used in clinical practice.

In this study, optic disc parameters presented with numerically better AUCs than RNFL thickness measurements. Three of the optic disc parameters measured by the OCT had the largest AUCs: average C/D ratio (0.958; 95% CI: 0.937–0.98; $P < 0.001$), vertical C/D ratio (0.957; 95% CI: 0.935–0.978; $P < 0.001$), and rim

area (0.952; 95% CI: 0.927–0.977; $P < 0.001$). Our results are among the best in the literature, especially considering that our glaucoma group basically comprised early glaucomatous eyes according to the Hodapp–Parrish–Anderson score (MD of HFA was − 5.42 ± 4.6 dB).[41] It is important to note, however, that patients were selected because of the optic disc appearance regardless of the VF or the OCT results, which may have biased the ONH parameters to be more accurate for differentiating between normal and eyes with glaucomatous optic neuropathy. Mwanza et al[13] found similar OCT diagnostic ability. They studied 73 glaucomatous eyes and 146 control eyes, and observed the largest AUCs for the rim area (0.912) and the vertical C/D ratio (0.890). This last parameter, vertical C/D ratio, had the best AUC (0.962) in a very similar study published by the same group that included 58 glaucomatous eyes and 99 controls.[42] A recent similar study[43] that included a large sample (209 glaucomatous eyes, 405 pre-perimetric glaucomatous eyes, and 109 controls) had worse results compared with our study and that of Mwanza et al[13] Only rim area presented a relatively good AUC and it was worse than that of the average RNFL thickness. One potential reason for this is that they included glaucomatous eyes at an earlier stage of the disease. Indeed, the diagnostic ability improved when advance glaucoma cases were selected. Pollet-Villard et al[32] reported similar results.

Many studies have confirmed the good diagnostic ability of peripapillary RNFL thickness measured by OCT.[11–13] In our study, the best AUC was for the RNFL thickness at the inferior quadrant (0.926; 95% CI: 0.894–0.958; $P < 0.001$), followed by the average RNFL thickness (0.918; 95% CI: 0.885–0.952; $P < 0.001$) and the RNFL thickness at the 7 clock-hour position (0.905; 95% CI: 0.869–0.940; $P < 0.001$). These three parameters also had the best AUCs in the Mwanza et al study.[13]

Comparison of measurements obtained by the Cirrus and Stratus OCT indicates that both tests have the same diagnostic ability despite the better reproducibility of the Cirrus OCT.[26,44,45] Most of the studies show consistency in the parameters with the best AUCs: RNFL thickness at the inferior quadrant, RNFL thickness at the 7 and 6 clock-hour positions, and average RNFL thickness.[40,46] These results support the idea that early glaucoma damage usually starts at the superior and inferior optic disc poles.[14,30,47,48]

In conclusion, the HFA, Octopus, and Cirrus OCT did not significantly differ in their ability to discriminate glaucomatous optic neuropathy. The three tests demonstrated very good diagnostic ability for discriminating between healthy and glaucomatous eyes.

Summary

What was known before
- Current knowledge of the relative diagnostic performance of both standard automated perimetries (Humphrey and Octopus) and OCT comes from studies in which the data were analyzed independently for each test, or where only one kind of VF was compared with a structural test.

What this study adds
- The main objective of this study was to compare the diagnostic ability of the most popular VF tests and spectral-domain OCT to differentiate between healthy individuals and patients with glaucomatous optic neuropathy. To the best of our knowledge, this is the first study that attempted to compare these tests.

Conflict of interest

The authors declare no conflict of interest.

References

1 Foster JP, Buhrman R, Quigley HA. The definition and classification of glaucoma in prevalence surveys. *Br J Ophthalmol* 2002; **86**: 238–242.

2 Kass MA, Heuer DK, Higginbotham EJ, Johnson CA, Keltner JL, Miller JP et al. The ocular hyper- tension treatment study: a randomized trial determines that topical ocular hypotensive medication delays or prevents the onset of primary open-angle glaucoma. *Arch Ophthalmol* 2002; **120**: 701–713.

3 European Glaucoma Prevention Study (EGPS) Group. Results of the European glaucoma prevention study. *Ophthalmology* 2005; **112**: 366–375.

4 Leung CK, Liu S, Weinreb RN, Lai G, Ye C, Cheung CY et al. Evaluation of retinal nerve fiber layer progression in glaucoma a prospective analysis with neuroretinal rim and visual field progression. *Ophthalmology* 2011; **118**: 1551–1557.

5 Gonzalez-Hernandez M, Pablo L, Armas-Dominguez K, Rodriguez de la Vega R, Ferreras A, Gonzalez et al. Structure-function relationship depends on glaucoma severity. *Br J Ophthalmol* 2009; **93**: 1195–1199.

6 López-Peña MJ, Ferreras A, Larrosa JM, Polo V, Pablo LE. Relationship between standard automated perimetry and retinal nerve fiber layer parameters obtained with optical coherence tomography. *J Glaucoma* 2011; **20**: 422–432.

7 Shah NN, Bowd C, Medeiros FA, Weinreb RN, Sample PA, Hoffmann EM et al. Combining structural and functional testing for detection of glaucoma. *Ophthalmology* 2006; **113**: 1593–1602.

8 Garway-Heath DF, Friedman DS. How should results from clinical tests be integrated into the diagnostic process? *Ophthalmology* 2006; **113**: 1479–1480.

9 Bengtsson B, Olsson J, Heijl A, Rootzén H. A new generation of algorithms for computerized threshold perimetry, SITA. *Acta Ophthalmol Scand* 1997; **75**: 368–375.

10 Morales J, Weitzman ML, González de la Rosa M. Comparison between tendency-oriented perimetry (TOP) and octopus threshold perimetry. *Ophthalmology* 2000; **107**: 134–142.

11 Leung CK, Choi N, Weireb RN, Liu S, Ye C, Liu L et al. Retinal nerve fiber layer imaging with spectral-domain optical coherence tomography pattern of RNFL defects in glaucoma. *Ophthalmology* 2010; **117**: 2337–2344.

12 Hwang YH, Kim YY. Glaucoma diagnostic ability of quadrant and clock-hour neuroretinal rim assessment using Cirrus HD optical coherence tomography. *Invest Ophthalmol Vis Sci* 2012; **53**: 2226–2234.

13 Mwanza JC, Oakley JD, Budenz DL, Anderson DR. Cirrus Optical Coherence Tomography Normative Database Study Group. Ability of Cirrus HD-OCT optic nerve head parameters to discriminate normal from glaucomatous eyes. *Ophthalmology* 2011; **118**: 241–248.

14 Ferreras A, Pablo LE, Pajarín AB, Larrosa JM, Polo V, Honrubia FM. Logistic regression analysis for early glaucoma diagnosis using optical coherence tomography. *Arch Ophthalmol* 2008; **126**: 465–470.

15 Bowd C, Hao J, Tavares IM, Medeiros FA, Zangwill LM, Lee TW et al. Bayesian machine learning classifiers for combining structural and functional measurements to classify healthy and glaucomatous eyes. *Invest Ophthalmol Vis Sci* 2008; **49**: 945–953.

16 Pablo LE, Ferreras A, Pajarin AB, Fogagnolo P. Diagnostic ability of a linear discriminant function for optic nerve head parameters measured with optical coherence tomography for perimetric glaucoma. *Eye* 2010; **24**: 1051–1057.

17 Leung CK, Cheung CY, Weinreb RN, Qiu Q, Liu S, Li H et al. Retinal nerve fiber layer imaging with spectral-domain optical coherence tomography: a variability and diagnostic performance study. *Ophthalmology* 2009; **116**: 1257–1263.

18 Gonzalez de la Rosa M, Gonzalez-Hernandez M, Garcia Feijoo J, Morales J, Azuara-Blanco A. Diagnostic accuracy and reproducibility of tendency oriented perimetry in glaucoma. *Eur J Ophthalmol* 2006; **16**: 259–267.

19 Birt CM, Shin DH, Samudrala V, Hughes BA, Kim C, Lee D. Analysis of reliability indices from Humphrey visual field tests in an urban glaucoma population. *Ophthalmology* 1997; **104**: 1126–1130.

20 Chang RT, Knight OJ, Feuer WJ, Budenz DL. Sensitivity and specificity of time-domain versus spectral-domain optical coherence tomography in diagnosing early to moderate glaucoma. *Ophthalmology* 2009; **116**: 2294–2299.

21 Pierre-Filho Pde T, Schimiti RB, de Vasconcellos JP, Costa VP. Sensitivity and specificity of frequency-doubling technology, tendency-oriented perimetry, SITA standard and SITA Fast perimetry in perimetrically inexperienced individuals. *Acta Ophthalmol Scand* 2006; **84**: 345–350.

22 Papp A, Kis K, Németh J. Conversion formulas between automated-perimetry indexes as measured by two different types of instrument. *Ophthalmologica* 2001; **215**: 87–90.

23 Wadood AC, Azuara-Blanco A, Aspinall P, Taguri A, King AJ. Sensitivity and specificity of frequency-doubling technology, tendency-oriented perimetry, and Humphrey Swedish interactive threshold algorithm-fast perimetry in a glaucoma practice. *Am J Ophthalmol* 2002; **133**: 327–332.

24 Ferreras A, Polo V, Larrosa JM, Pablo LE, Pajarín AB, Pueyo V et al. Can frequency-doubling technology and short-wavelength automated perimetries detect visual field defects before standard automated perimetry in patients with pre-perimetric glaucoma? *J Glaucoma* 2007; **16**: 372–383.

25 Fogagnolo P, Rossetti L, Ranno S, Ferreras A, Orzalesi N. Short-wavelength automated perimetry and frequency-doubling technology perimetry in glaucoma. *Prog Brain Res* 2008; **173**: 101–124.

26 Racette L, Chiou CY, Hao J, Bowd C, Goldbaum MH, Zangwill LM *et al*. Combining functional and structural tests improves the diagnostic accuracy of relevance vector machine classifiers. *J Glaucoma* 2010; **19**: 167–175.

27 Horn FK, Mardin CY, Bendchneider D, Jünemann AG, Adler W, Tornow RP. Frequency doubling technique perimetry and spectral domain optical coherence tomography in patients with early glaucoma. *Eye* 2011; **25**: 17–29.

28 Garway-Heath DF, Poinoosawmy D, Fitzke FW, Hitchings RA. Mapping the visual field to the optic disc in normal tension glaucoma eyes. *Ophthalmology* 2000; **107**: 1809–1815.

29 Gardiner SK, Johnson CA, Cioffi GA. Evaluation of the structure-function relationship in glaucoma. *Invest Ophthalmol Vis Sci* 2005; **46**: 3712–3717.

30 Bowd C, Zangwill LM, Medeiros FA, Tavares IM, Hoffmann EM, Bourne RR *et al*. Structure-function relationships using confocal scanning laser ophthalmoscopy, optical coherence tomography, and scanning laser polarimetry. *Invest Ophthalmol Vis Sci* 2006; **47**: 2889–2895.

31 Ferreras A, Pablo LE, Garway-Heath DF, Fogagnolo P, García-Feijoo J. Mapping standard automated perimetry to the peripapillary retinal nerve fiber layer in glaucoma. *Invest Ophthalmol Vis Sci* 2008; **49**: 3018–3025.

32 Pollet-Villard F, Chiquet C, Romanet JP, Noel C, Aptel F. Structure-function relationships with spectral-domain optical coherence tomography retinal nerve fiber layer and optic nerve head measurements. *Invest Ophthalmol Vis Sci* 2014; **55**: 2953–2962.

33 Monsalve B, Ferreras A, Khawaja AP, Calvo P, Ara M, Fogagnolo P *et al*. The relationship between structure and function as measured by OCT and Octopus perimetry. *Br J Ophthalmol* 2015; **99**: 1230–1235.

34 Chylack LT Jr, Wolfe JK, Singer DM, Leske MC, Bullimore MA, Bailey IL *et al*. The lens opacities classification system III. the longitudinal study of cataract study group. *Arch Ophthalmol* 1993; **111**: 831–836.

35 DeLong ER, DeLong DM, Clarke-Pearson DL. Comparing the areas under two or more correlated receiver operating characteristic curves: a nonparametric approach. *Biometrics* 1988; **44**: 837–845.

36 Artes PH, O'Leary N, Hutchison DM, Heckler L, Sharpe GP, Nicolela MT *et al*. Properties of the statpac visual field index. *Invest Ophthalmol Vis Sci* 2011; **52**: 4030–4038.

37 Nascimento VC, Kasahara N, Cohen R, Almeida GV, Mandia C Jr, Paolera MD *et al*. Location and frequency of visual field defects as measured by SITA (Swedish Interactive Threshold Algorithm) strategy in primary open angle glaucoma. *Arq Bras Oftalmol* 2005; **68**: 661–665.

38 Lau LI, Liu CJ, Chou JC, Hsu WM, Liu JH. Patterns of visual field defects in chronic angle-closure glaucoma with different disease severity. *Ophthalmology* 2003; **110**: 1890–1894.

39 Schiefer U, Papageorgiou E, Sample PA, Pascual JP, Selig B, Krapp E *et al*. Spatial pattern of glaucomatous visual field loss obtained with regionally condensed stimulus arrangements. *Invest Ophthalmol Vis Sci* 2010; **51**: 5685–5689.

40 Sihota R, Gupta V, Tuli D, Sharma A, Sony P, Srinivasan G. Classifying patterns of localized glaucomatous visual field defects on automated perimetry. *J Glaucoma* 2007; **16**: 146–152.

41 Hodapp E, Parrish RK II, Anderson DR. *Clinical Decisions in Glaucoma*. Mosby: St Louis, MO, USA, 1993; 52–61.

42 Mwanza JC, Durbin MK, Budenz DL, Sayyad FE, Chang RT, Neelakantan A *et al*. Glaucoma diagnostic accuracy of ganglion cell-inner plexiform layer thickness: comparison with nerve fiber layer and optic nerve head. *Ophthalmology* 2012; **119**: 1151–1158.

43 Sung KR, Na JH, Lee Y. Glaucoma diagnostic capabilities of optic nerve head parameters as determined by Cirrus HD optical coherence tomography. *J Glaucoma* 2012; **21**: 498–504.

44 Chen HY, Chang YC, Wang IJ, Chen WC. Comparison of glaucoma diagnoses using stratus and Cirrus optical coherence tomography in different glaucoma types in a Chinese population. *J Glaucoma* 2013; **22**(8): 638–646.

45 Moreno-Montañés J, Olmo N, Alvarez A, García N, Zarranz-Ventura J. Cirrus high-definition optical coherence tomography compared with stratus optical coherence tomography in glaucoma diagnosis. *Invest Ophthalmol Vis Sci* 2010; **51**: 335–343.

46 Chen HY, Chang YC. Meta-analysis of stratus OCT glaucoma diagnostic accuracy. *Optom Vis Sci* 2014; **91**: 1129–1139.

47 Uchida H, Brigatti L, Caprioli J. Detection of structural damage from glaucoma with confocal laser image analysis. *Invest Ophthalmol Vis Sci* 1996; **37**: 2393–2401.

48 Pablo LE, Ferreras A, Fogagnolo P, Figus M, Pajarín AB. Optic nerve head changes in early glaucoma: a comparison between stereophotography and Heidelberg retina tomography. *Eye* 2010; **24**: 123–130.